

TO THE EDITOR:

A novel transmembrane *CXCR4* variant that expands the WHIM genotype-phenotype paradigm

Katarina Zmajkovicova,^{1,*} Sumit Pawar,^{2,*} Svetlana O. Sharapova,³ Christoph B. Geier,^{4,5} Ivana Wiest,² Chi Nguyen,¹ Halenya Monticelli,¹ Sabine Maier-Munsa,² Kelly Chen,⁶ John W. Sleasman,⁷ Svetlana Aleshkevich,³ Ekaterina Polyakova,³ Inga Sakovich,³ Klaus Warnatz,^{4,5} Bodo Gribbacher,^{4,5} Michele Proietti,^{8,9} Neal Sondheimer,¹⁰ Boglarka Ujhazi,¹¹ Sumai Gordon,¹¹ Maryssa Ellison,¹¹ Melis Yilmaz,^{11,12} Jolan E. Walter,¹¹⁻¹³ Adriana Badarau,² Arthur G. Taveras,⁶ Jadee L. Neff,¹⁴ Jacob R. Bledsoe,¹⁵ and Teresa K. Tarrant^{16,17}

¹X4 Pharmaceuticals (Austria) GmbH, Vienna, Austria; ²Formerly X4 Pharmaceuticals (Austria) GmbH, Vienna, Austria; ³Research Department, Belarusian Research Center for Pediatric Oncology, Hematology, and Immunology, Minsk, Belarus; ⁴Department of Rheumatology and Clinical Immunology and ⁵Center for Chronic Immunodeficiency, University Medical Center Freiburg, Faculty of Medicine, University of Freiburg, Freiburg, Germany; ⁶X4 Pharmaceuticals, Boston, MA; ⁷Division of Allergy, Immunology, Department of Pediatrics, Duke University School of Medicine, Durham, NC; ⁸Department of Rheumatology and Clinical Immunology and ⁹RESIST-Cluster of Excellence 2155, Hannover Medical School, Hannover, Germany; ¹⁰Department of Molecular Genetics, University of Toronto, Toronto, ON, Canada; ¹¹Division of Allergy and Immunology, Department of Medicine, Johns Hopkins All Children's Hospital, St Petersburg, FL; ¹²Division of Allergy & Immunology, Department of Pediatrics, Morsani College of Medicine, University of South Florida, Tampa, FL; ¹³Division of Allergy and Immunology, Massachusetts General Hospital for Children, Boston, MA; ¹⁴Division of Hematopathology, Department of Pathology, Duke University, Durham, NC; ¹⁵Department of Pathology, Boston Children's Hospital, Boston, MA; ¹⁶Division of Rheumatology and Immunology, Department of Medicine, Duke University, Durham, NC; and ¹⁷Durham Veterans Affairs Medical Center, Durham, NC

Variants in the C-X-C motif chemokine receptor 4 gene (*CXCR4*) are associated with a rare autosomal-dominant combined immunodeficiency, WHIM (warts, hypogammaglobulinemia, infections, and myelokathexis) syndrome.^{1,2} The *CXCR4*/C-X-C motif chemokine ligand 12 (*CXCL12*) axis is a master regulator of immune cell bone marrow homing and egress³⁻⁵ and B-cell development.⁶ Previously known pathogenic nonsense, frameshift, and missense variants identified in individuals with WHIM syndrome (*CXCR4*^{WHIM}) have been localized to the intracellular C-terminal region of *CXCR4*, a G protein-coupled receptor.² We describe 4 unrelated patients, designated P1 to P4, with variable clinical presentations including leukopenia, hypercellular bone marrow, recurrent infections, hypogammaglobulinemia, and susceptibility to human papillomavirus, harboring a novel heterozygous *CXCR4* variant (c.250G>C; p.D84H), designated as *CXCR4*^{D84H}, in the second transmembrane domain of the receptor. We performed comprehensive *ex vivo* and *in vitro* functional characterization of cells harboring *CXCR4*^{D84H} in parallel with *in silico* molecular modeling to determine pathogenicity of the newly discovered variant. See supplemental Methods for detailed methods, including supplemental Table 1A-B.

The studies were approved by institutional review board (IRB) of the respective institutions, including institutional review of Duke University (IRB number Pro00066839), Belarusian Research Center for Pediatric Oncology (IRB number 200809-RD), and University Medical Center Freiburg (IRB number 354/19).

Table 1 and supplemental Table 2A summarize the clinical and laboratory characteristics and immunophenotyping data for P1 to P4.

P1 is a female aged 40 years with plantar warts since childhood, recurrent vulvovaginal and anal dysplasia, and carcinoma in situ for 20 years. Cytopenia, including neutropenia, were first documented at age 15 years. She had Epstein-Barr virus in childhood from which she recovered and was

Submitted 6 October 2023; accepted 22 April 2024; prepublished online on *Blood Advances* First Edition 20 May 2024; final version published online 12 July 2024.
<https://doi.org/10.1182/bloodadvances.2023011875>.

*K.Z. and S.P. contributed equally to this study.

The data that support the *in vitro* experimental findings and molecular dynamics simulations in this study are available from the corresponding author upon reasonable request. Qualified scientific and medical researchers may make requests for clinical trial data that underlie the results (text, tables, figures) reported in this article, after de-identification, at medicalinfo@x4pharma.com. Methodologically sound proposals for such data will be evaluated and approved by X4 Pharmaceuticals, Inc in its sole

discretion. All approved researchers must sign a data access agreement prior to accessing the data. Data will be available as soon as possible but no later than within 1 year of the acceptance of the article for publication, and for 3 years after article publication. X4 Pharmaceuticals, Inc. will not share identified participant data or a data dictionary.

The full-text version of this article contains a data supplement.

© 2024 by The American Society of Hematology. Licensed under [Creative Commons Attribution-NonCommercial-NoDerivatives 4.0 International \(CC BY-NC-ND 4.0\)](https://creativecommons.org/licenses/by-nc-nd/4.0/), permitting only noncommercial, nonderivative use with attribution. All other rights reserved.

Table 1. Summary of patient phenotypes including main clinical manifestations and laboratory features in 4 patients harboring missense variant CXCR4^{D84H}

	P1	P2*	P3	P4	Reference ranges		
Characteristics							
CXCR4 variant	c.250G>C (p.D84H) heterozygous	c.250G>C (p.D84H) heterozygous	c.250G>C (p.D84H) heterozygous	c.250G>C (p.D84H) heterozygous			
Sex at birth	Female	Male	Male	Female			
Age, y	40	13	3, died	67			
Hemogram, x10⁹/L†					1-6 y	12-18 y	18+ y
WBC	2.2-3.9	0.68-6.03	13.3	8.08	5.0-17.0	4.5-13.0	3.2-9.8
Neutrophils	0.6-1.2	0.16-2.79	8.9	4.93	1.0-8.5	1.5-8.0	1.56-6.45
Lymphocytes	1.5-2.1	0.43-2.55	2.9	2.49	1.5-9.5	1.1-4.5	0.95-3.07
Monocytes	0-0.1	0.07-0.52	1.07	0.5	0.2-1.0	0.2-1.0	0.24-0.86
Platelets	144-166	53-268	54	298	150-400	150-400	150-450
Serum immunoglobulin, mg/dL‡					2 to <4 y	10 to <13 y	18+ y
IgG	1060	650	858-982	403	295-1156	503-1719	767-1590
IgG1	§	§	§	200	158-721	280-1030	341-894
IgG2	§	§	§	156	39-176	66-502	171-632
IgG3	§	§	§	37	17-84.7	11.5-105.3	18.4-106
IgG4	§	§	§	5.2	0.4-49.1	1.0-121.9	2.4-121.0
IgM	109	54	67-81	81	27-246	42-295	61-356
IgA	94	162	61-98	98	37-184	41-255	37-278
Tetanus antibody titer, IU/mL	5.22	§	§	1.41		>0.16	>0.16
Pneumococcal antibody titers, µg/mL	21/23 serotypes >1.3	§	§	§		>1.3	>1.3
Clinical presentation							
Bone marrow	Hypocellular (20%-30%) with mild granulocytic hypoplasia, hypolobulated megakaryocytes, bilobed neutrophils, and granulocyte precursors	Increased cellularity, 64% of cells are represented by neutrophils of varying degrees of maturity	ITP; punctate is rich; there are many megakaryocytes, but no functioning	§			
Warts	Hands, feet, and anogenital	(-)	(-)	(-)			
Infections	EBV, HPV, and H1N1 pneumonia	HSV, parvovirus, SARS-CoV-2, pneumonia (<i>Bacillus cereus</i> , <i>Pseudomonas</i> species), and diarrhea (<i>Candida</i>)	Seroconverted for CMV and EBV, HSV	URTI			
Malignancy	Anal intraepithelial neoplasia grade 3, cervical carcinoma in situ, high-grade vulval intraepithelial neoplasia, and anal dysplasia	(-)	(-)	(-)			
Other		Autoimmune thyroiditis					
Prior treatments							
Immunoglobulin therapy	(-)	(+)	(+)	(+)			
G-CSF	(-)	(-)	(-)	(-)			
Antibiotics	Rare	(+)	(+)	(+); prophylaxis			
Other	Cidofovir for AIN3						
Family history	Family members decline genetic testing. No clinically affected family members	Mother harbors D84H; healthy	Not known	(-)			

Values not within the normal range are shown in bold font.

AIN3, anal intraepithelial neoplasia grade 3; CMV, cytomegalovirus; EBV, Epstein-Barr virus; G-CSF, granulocyte colony-stimulating factor; H1N1, influenza A virus subtype H1N1; HPV, human papillomavirus; HSV, herpes simplex virus; ITP, immune thrombocytopenia; SARS-CoV-2, severe acute respiratory syndrome coronavirus 2; URTI, upper respiratory tract infection; WBC, white blood cell.

*The range for P2 is based on 2 different time points: 2020 and 2021.

†Hemogram reference ranges for <18 years and >18 years of age are based on cutoffs provided by North Bristol National Health Service and Cleveland Clinic, respectively.

‡Serum immunoglobulin references ranges are based on cutoffs provided by Mayo Clinic Laboratories.

§No data.

hospitalized briefly for influenza-related pneumonia. P1 has normal immunoglobulin levels. Peripheral blood smear (supplemental Figure 1A) showed hypolobated neutrophils, not typical of myelokathexis.

P2 is a male aged 12 years with trilineage leukopenia, transient thrombocytopenia, recurrent infections, and autoimmune thyroiditis but no warts or hypogammaglobulinemia. His bone marrow biopsy showed abnormal neutrophil retention without classic myelokathexis neutrophil morphology (supplemental Figure 1B). P2's mother shares the genetic variation but is healthy (supplemental Table 2B).

Limited information is known about P3, a male who died at age 3 years from infectious complications leading to multiple organ failures. He had recurrent infections and was suspected to have immune thrombocytopenic purpura. He did not have peripheral blood leukopenia, although peripheral blood sampling may have occurred during active infection. Family history of P3 and P4 are unknown.

P4 is a female aged 67 years with hypogammaglobulinemia. Immunoglobulin G (IgG) level was 403 mg/dL, and IgG1 subclass was 200 mg/dL; other immunoglobulins were normal. She had upper respiratory tract infections that ceased after IgG replacement therapy initiation and rosacea treated with doxycycline. She does not have cytopenia or human papillomavirus.

The probands are nonrelated from nonconsanguineous unions and were identified from 3 separate countries. All are heterozygous for *CXCR4* (c.250G>C), resulting in a single amino acid substitution, D84H. The missense variant is in a highly evolutionarily conserved region in the second transmembrane helix of the receptor (supplemental Figure 1C-D). ClinVar (VCV000808804.12) classified D84H as a variant of uncertain significance. In silico algorithms characterize D84H as deleterious (SIFT score, 0; CADD score, 26.8), probably damaging (PolyPhen2 score, 1) and likely disease causing (REVEL score, 0.951).

Impaired *CXCR4* receptor internalization, amplified signaling responsiveness, and enhanced migration are hallmarks of immune cells expressing *CXCR4*^{WHIM} receptors.⁷⁻¹⁰ CXCL12-induced *CXCR4* internalization was impaired in peripheral blood mononuclear cells (PBMCs) from P1, P2, and P4 compared with healthy donors (HDs; Figure 1A; supplemental Figure 2A-B). The findings prompted comparative studies of *CXCR4*^{D84H} with *CXCR4*^{R334X}, the most common and best-studied *CXCR4*^{WHIM} variant,² and *CXCR4*^{E343K}, the only known pathogenic missense variant.⁸ The *CXCR4*-negative K562 cell line⁹ was transfected to express aforementioned *CXCR4* variants for quantitative comparison of variant receptor function (supplemental Figure 2C). *CXCR4*^{D84H} showed impaired CXCL12-induced receptor internalization (Figure 1B; supplemental Figure 2D) similar to *CXCR4*^{E343K}. P1 and P2 lymphocyte subpopulations showed enhanced chemotaxis to CXCL12 relative to HDs across tested concentrations (Figure 1C; supplemental Figure 2E), similar to transfected K562 cells expressing *CXCR4*^{D84H} and other *CXCR4*^{WHIM} variants compared with K562-*CXCR4*^{WT} (Figure 1D). *CXCR4*^{R334X} and *CXCR4*^{E343K} showed significant increase in pAKT and pERK levels after CXCL12 stimulation compared with *CXCR4*^{WT}, confirming previous findings^{9,10}; however, no enhancement was observed in pAKT or pERK levels in P1 lymphocytes or K562-*CXCR4*^{D84H} (supplemental Figure 2F-I). Ca²⁺ mobilization was impaired in P1

PBMCs after CXCL12 stimulation compared with HDs (Figure 1E). This phenotype was confirmed in K562-*CXCR4*^{D84H}, in which the maximum efficacy of CXCL12 to mobilize calcium decreased to 46%. In contrast, K562-*CXCR4*^{R334X} and K562-*CXCR4*^{E343K} showed ~1.2-fold increased Ca²⁺ mobilization compared with K562-*CXCR4*^{WT} (Figure 1F). Similar results were obtained when cyclic adenosine monophosphate (cAMP) inhibition was measured in K562-*CXCR4*^{D84H} compared with K562-*CXCR4*^{R334X} and K562-*CXCR4*^{E343K} (Figure 1G). In summary, signaling responses of *CXCR4*^{D84H} are distinct from other *CXCR4*^{WHIM} variants.

D84 is a critical, conserved residue of the sodium ion binding pocket, essential for signaling of class A G protein-coupled receptors.^{11,12} Though crystal structures of *CXCR4* show no Na⁺ ion in this location,^{13,14} site-directed mutagenesis and molecular dynamics studies support its presence.¹⁵⁻¹⁷ We performed molecular dynamics simulations analyzing the D84H variant structure, given the change in amino acid charge from negative D to neutral H. Simulations suggested a collapse of the Na⁺ ion binding pocket, destabilized inactive state, and potential constitutive activity (CA) of a more thermodynamically preferred active-form *CXCR4*^{D84H} configuration (supplemental Figures 3A-C and 4). To test this hypothesis, *CXCR4*^{D84H} activity was analyzed under basal conditions. In K562-*CXCR4*^{WT}, CXCL12 addition led to inhibition of forskolin-stimulated cAMP production, typical for G_{αi}-coupled receptors (supplemental Figure 3D). In K562-*CXCR4*^{D84H}, cAMP production was already suppressed in absence of CXCL12, indicative of constitutive G_{αi} activation. In line with *CXCR4*^{D84H} effects, other previously known CA *CXCR4* variants exhibited enhanced chemotactic CXCL12 response.¹⁸ Due to the already high receptor basal activity, CA *CXCR4* cannot be further stimulated with CXCL12 and show decreased responses in ligand-induced calcium mobilization.¹⁷ These observations explained the decreased signaling observed with *CXCR4*^{D84H} in calcium mobilization and cAMP assays.

CXCR4^{D84H} represents a novel disease-causing variant with distinct functional properties that could mechanistically explain the phenotypic differences of P1 to P4 compared with previously described C-terminal variants. Patients with WHIM syndrome display variable phenotypes and incomplete penetrance of the classic tetrad,^{2,19} and the *CXCR4*^{D84H} patients described have milder infections, cytopenia, and hypogammaglobulinemia. Further, 3 of 4 patients had thrombocytopenia, and 2 of 4 displayed low natural killer cell counts, less typical for WHIM syndrome.

Mavoxifafor, a small-molecule *CXCR4* antagonist,^{20,21} inhibited CXCL12 binding with comparable potency (IC₅₀, 3.9-5.6 nM) across K562-*CXCR4*^{D84H}, K562-*CXCR4*^{R334X}, K562-*CXCR4*^{E343K}, and K562-*CXCR4*^{WT} (supplemental Figure 5A). Mavoxifafor abrogated enhanced CXCL12-induced chemotaxis in patient-derived lymphocytes (supplemental Figure 5B-E). P1 was enrolled in a phase 1b/2 open-label trial evaluating safety, tolerability, and early efficacy of mavoxifafor (400 mg once daily) across chronic neutropenic disorders (NCT04154488).²² Hematologic parameter monitoring showed increased white blood cell count, absolute neutrophil count, and absolute lymphocyte count on day 1 of mavoxifafor treatment (maximum fold change of 2.55, 2.52, and 2.64 respectively; X4, unpublished data, 20 September 2022; Figure 1H). Thus, we propose that mavoxifafor may be considered a potential leukopenia treatment in *CXCR4*^{D84H} patients.

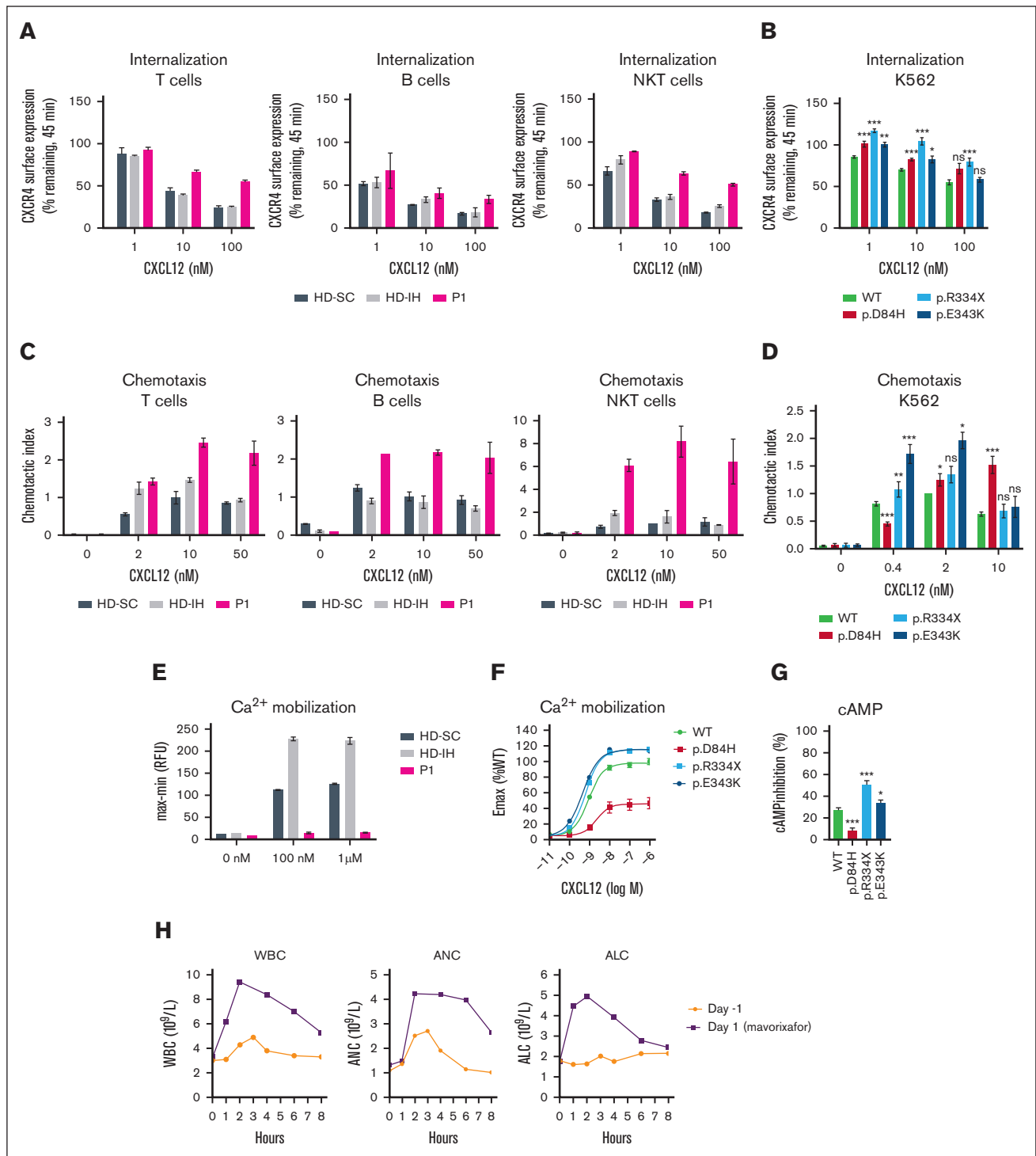


Figure 1. Impact of CXCR4^{D84H} on receptor function and effects of mavoxixafor treatment in P1. (A) PBMCs isolated from HDs (HD-SC and HD-IH) and P1 were stimulated with CXCL12 (vehicle, 1 nM, 10 nM, and 100 nM) for 45 minutes. CXCR4 receptor internalization was assessed by surface expression of CXCR4 by flow cytometry. Values are expressed as percent of remaining CXCR4 expression compared with vehicle-treated cells. PBMCs were subtyped using fluorescent mAbs specific for CD3 (T cells), CD19 (B cell), and CD3 and CD56 (NKT cells). Statistical analysis was not performed owing to low sample numbers. Mean \pm standard deviation (SD) of 2 to 4 from 2 biological replicates. (B) K562 cells were transiently transfected with indicated CXCR4 constructs and stimulated with CXCL12 (vehicle, 1 nM, 10 nM, and 100 nM) for 45 minutes. CXCR4 receptor internalization was assessed by surface expression of CXCR4 via flow cytometry. Statistical significance determined by Mann-Whitney tests comparing variants with the WT at each respective concentration of ligand. Values are expressed as percent of remaining CXCR4 compared with vehicle-treated cells. Values represent mean \pm standard error of mean (SEM) of 3 to 17. * P < .05; ** P < .01; *** P < .001. (C) Transwell chemotaxis assay: PBMCs isolated from HDs (HD-SC and HD-IH) and P1 migrated toward 2, 10, and 50 nM CXCL12 or medium only for 2.5 hours. The total number of migrated cells was normalized to the HD-SC with 10 nM CXCL12 in each cell type. PBMCs were subtyped

Figure 1 (continued) using fluorescent mAbs specific for CD3 (T cells), CD19 (B cell), and CD3 and CD56 (NKT cells). Statistical analysis in PBMCs was not performed owing to low sample numbers. Mean \pm SD of 2. (D) Transwell chemotaxis assay: K562 cells transiently transfected with indicated CXCR4 constructs migrated toward 0.4, 2, and 10 nM CXCL12 or medium only for 4 hours. The total number of migrated cells was normalized to WT with 2 nM CXCL12 in each assay. Statistical significance was determined by Mann-Whitney tests (0.4 nM and 10 nM) and 1-sample Wilcoxon signed-rank test (2 nM) comparing variants with the WT at each respective concentration of ligand. Mean \pm SEM of 5 to 20. * $P < .05$; ** $P < .01$; *** $P < .001$. (E) PBMCs isolated from HDs (HD-SC and HD-IH) and P1 were stimulated with vehicle, 100 nM or 1 μ M CXCL12 to measure Ca^{2+} mobilization. Statistical analysis was not performed owing to low sample numbers; $n = 2$ technical replicates; the experiment is representative of 2 independent experiments. (F) K562 cells with stable CXCR4 expression were stimulated with serial dilutions of CXCL12 to measure Ca^{2+} mobilization. Relative fluorescence units measured in WT-expressing cell line at 1 μ M CXCL12 represented 100%. Mean \pm SEM of 11 to 12. (G) K562 cells with stable CXCR4 expression were stimulated with forskolin \pm 100 nM CXCL12 for 30 minutes. cAMP production was measured by enzyme-linked immunosorbent assay. Percent of inhibition of cAMP production by CXCL12 was calculated relative to forskolin-only treated cells. Statistical significance was determined by Mann-Whitney tests comparing variants with the WT. Values represent mean \pm SEM of 9 to 12. * $P < .05$; ** $P < .01$; *** $P < .001$. (H) Time course of WBC counts, ANC, and ALC for P1 before receiving oral mavorixafor (day -1) and on the first day of mavorixafor treatment (day 1). ALC, absolute lymphocyte count; AMC, absolute monocyte count; ANC, absolute neutrophil count; CD, cluster of differentiation; HD-IH, healthy donor in-house; HD-SC, healthy donor shipping control; mAb, monoclonal antibody; NK, natural killer; NKT, natural killer T; ns, not significant; WBC, white blood cell; WT, wild type.

The average CXCR4 (c.250G>C) allele frequency suggests 7.5 per 100 000 individuals may harbor CXCR4^{D84H} (supplemental Table 3). The relatively high allele frequency, P4's later symptom onset age, and P2's healthy mother harboring CXCR4^{D84H} suggest incomplete penetrance and/or variable expressivity of the CXCR4^{D84H} phenotype.

Our observations from CXCR4^{D84H} patients and results of the functional characterization of PBMCs and cells expressing the D84H variant highlight several novel findings, expanding the current understanding of genotype-phenotype correlations within the CXCR4 landscape.

Acknowledgments: The authors thank patients and their families for their participation and acknowledge the contributions of Richard Pollison to the chronic neutropenic disorders clinical trial. Molecular dynamics simulations were performed by Jian Yin and Junkun Lei at WuXi AppTec. Biostatistical consulting was provided by Precision for Medicine, Gladstone, New Jersey, and medical writing assistance was provided by Jane Nguyen of PRECISIONscientia in Yardley, Pennsylvania, which was supported financially by X4 Pharmaceuticals, Inc, in compliance with international Good Publication Practice guidelines.

The biorepository for processing and storing blood specimens was supported by a grant from the Jeffrey Modell Foundation. B.G. is funded by the Deutsche Forschungsgemeinschaft (GR1617/14-1/iPAD; SFB1160/2_B5; RESIST-EXC 2155 [project ID 390874280]; and the EU-H2020-MSCA-COFUND EURIdoc programme [number 101034170]) and the Bundesministerium für Bildung und Forschung (GAIN O1GM1910A).

Contribution: K.Z., S.P., C.N., and A.B. designed the study; S.O.S., C.B.G., K.C., J.W.S., S.A., E.P., I.S., K.W., B.G., M.P., J.R.B., and T.K.T. provided patient data and samples; K.Z., S.P., C.B.G., I.W., C.N., B.U., H.M., S.M.-M., K.C., B.G., M.P., S.G., and J.L.N. acquired and generated data; K.Z., S.P., C.B.G., C.N., M.E., J.E.W., A.B., J.L.N., N.S., and T.K.T. analyzed and interpreted the results; K.Z., S.P., C.B.G., J.E.W., A.G.T., and T.K.T. assisted in the writing and editing of the manuscript; and all authors read and approved the submitted version of the manuscript.

Conflict-of-interest disclosure: X4 Pharmaceuticals funded the development of this manuscript. T.K.T. is a principal investigator in the phase 3 trial of mavorixafor for WHIM syndrome and consultant to X4 Pharmaceuticals. N.S. is a consultant to X4 Pharmaceuticals. K.Z., C.N., H.M., K.C., and A.G.T. are employees, and K.Z., C.N.,

H.M., and A.G.T. hold shares of X4 Pharmaceuticals. A.B., S.P., S.M.-M., and I.W. hold shares of X4 Pharmaceuticals. J.E.W. has received funding for investigator initiated and sponsored clinical trials from X4 Pharmaceuticals; served as consultant to X4 Pharmaceuticals in the past; and is a principal investigator of investigator-initiated and sponsored studies funded by X4 Pharmaceuticals. J.L.N. serves as a speaker for EUSA Pharma; an adviser for EUSA Pharma and AbbVie; and a consultant for Guidepoint Global. The remaining authors declare no competing financial interests.

ORCID profiles: K.Z., 0000-0002-1394-7039; S.O.S., 0000-0003-1390-2348; C.B.G., 0000-0003-4353-8663; H.M., 0000-0001-6972-8698; E.P., 0000-0002-0706-6622; K.W., 0000-0002-1172-865X; B.G., 0000-0002-6897-6806; M.Y., 0000-0002-8506-7372; J.E.W., 0000-0002-6192-0703; J.L.N., 0000-0002-4924-4247; J.R.B., 0000-0002-2387-5462; T.K.T., 0000-0003-4067-5363.

Correspondence: Katarina Zmajkovicova, X4 Pharmaceuticals (Austria) GmbH, Helmut-Qualtinger-Gasse 2, 1030 Vienna, Austria; email: katarina.zmajkovicova@x4pharma.com; and Teresa K. Tarrant, Duke University Medical Center 3874, 200 Trent Dr, Durham, NC 27710; email: teresa.tarrant@duke.edu.

References

- Hernandez PA, Gorlin RJ, Lukens JN, et al. Mutations in the chemokine receptor gene CXCR4 are associated with WHIM syndrome, a combined immunodeficiency disease. *Nat Genet.* 2003;34(1):70-74.
- Heusinkveld LE, Majumdar S, Gao JL, McDermott DH, Murphy PM. WHIM syndrome: from pathogenesis towards personalized medicine and cure. *J Clin Immunol.* 2019;39(6):532-556.
- Levy E, Reger R, Segerberg F, et al. Enhanced bone marrow homing of natural killer cells following mRNA transfection with gain-of-function variant CXCR4^{R334X}. *Front Immunol.* 2019;10:1262.
- Beck TC, Gomes AC, Cyster JG, Pereira JP. CXCR4 and a cell-extrinsic mechanism control immature B lymphocyte egress from bone marrow. *J Exp Med.* 2014;211(13):2567-2581.
- De Filippo K, Rankin SM. CXCR4, the master regulator of neutrophil trafficking in homeostasis and disease. *Eur J Clin Invest.* 2018;48 suppl 2(suppl 2):e12949.
- Ma Q, Jones D, Borghesani PR, et al. Impaired B-lymphopoiesis, myeloopoiesis, and derailed cerebellar neuron migration in CXCR4- and

- SDF-1-deficient mice. *Proc Natl Acad Sci U S A*. 1998;95(16): 9448-9453.
7. Balabanian K, Lagane B, Pablos JL, et al. WHIM syndromes with different genetic anomalies are accounted for by impaired CXCR4 desensitization to CXCL12. *Blood*. 2005;105(6): 2449-2457.
 8. Liu Q, Chen H, Ojode T, et al. WHIM syndrome caused by a single amino acid substitution in the carboxy-tail of chemokine receptor CXCR4. *Blood*. 2012;120(1):181-189.
 9. McDermott DH, Lopez J, Deng F, et al. AMD3100 is a potent antagonist at CXCR4 R334X, a hyperfunctional mutant chemokine receptor and cause of WHIM syndrome. *J Cell Mol Med*. 2011; 15(10):2071-2081.
 10. Zmajkovicova K, Pawar S, Maier-Munsa S, et al. Genotype-phenotype correlations in WHIM syndrome: a systematic characterization of CXCR4(WHIM) variants. *Genes Immun*. 2022; 23(6):196-204.
 11. Katritch V, Fenalti G, Abola EE, Roth BL, Cherezov V, Stevens RC. Allosteric sodium in class A GPCR signaling. *Trends Biochem Sci*. 2014;39(5):233-244.
 12. Zhou Q, Yang D, Wu M, et al. Common activation mechanism of class A GPCRs. *Elife*. 2019;8:e50279.
 13. Qin L, Kufareva I, Holden LG, et al. Structural biology. Crystal structure of the chemokine receptor CXCR4 in complex with a viral chemokine. *Science*. 2015;347(6226):1117-1122.
 14. Wu B, Chien EY, Mol CD, et al. Structures of the CXCR4 chemokine GPCR with small-molecule and cyclic peptide antagonists. *Science*. 2010;330(6007):1066-1071.
 15. Cong X, Golebiowski J. Allosteric Na(+)-binding site modulates CXCR4 activation. *Phys Chem Chem Phys*. 2018;20(38):24915-24920.
 16. Selvam B, Shamsi Z, Shukla D. Universality of the sodium ion binding mechanism in class A G-protein-coupled receptors. *Angew Chem Int Ed Engl*. 2018;57(12):3048-3053.
 17. Zhang WB, Navenot JM, Haribabu B, et al. A point mutation that confers constitutive activity to CXCR4 reveals that T140 is an inverse agonist and that AMD3100 and ALX40-4C are weak partial agonists. *J Biol Chem*. 2002;277(27):24515-24521.
 18. Sharma M, Afrin F, Tripathi R, Gangenahalli G. Regulated expression of CXCR4 constitutive active mutants revealed the up-modulated chemotaxis and up-regulation of genes crucial for CXCR4 mediated homing and engraftment of hematopoietic stem/progenitor cells. *J Stem Cells Regen Med*. 2013;9(1):19-27.
 19. Geier CB, Ellison M, Cruz R, et al. Disease progression of WHIM syndrome in an international cohort of 66 pediatric and adult patients. *J Clin Immunol*. 2022;42(8):1748-1765.
 20. Dale DC, Firkin F, Bolyard AA, et al. Results of a phase 2 trial of an oral CXCR4 antagonist, mavoxixafor, for treatment of WHIM syndrome. *Blood*. 2020;136(26):2994-3003.
 21. Efficacy and safety study of mavoxixafor in participants with Warts, Hypogammaglobulinemia, Infections, and Myelokathexis (WHIM) syndrome. ClinicalTrials.gov identifier: NCT03995108. Updated 6 October. 2023. Accessed 27 November 2023. <https://clinicaltrials.gov/study/NCT03995108?term=NCT03995108&rank=1>
 22. A study of mavoxixafor in participants with congenital neutropenia and chronic idiopathic neutropenia disorders. ClinicalTrials.gov identifier: NCT04154488. Updated 5 December. 2022. Accessed 29 December 2022. <https://clinicaltrials.gov/ct2/show/NCT04154488>